Korean J. Chem. Eng., 38(12), 2530-2535 (2021)
DOI: 10.1007/s11814-021-0887-0

pISSN: 0256-1115
eISSN: 1975-7220

Fabrication of transparent superhydrophobic polydimethylsiloxane elastomer by controlling the degree of combustion using thermal convection

Eungjun Lee and Do Hyun Kim†

Department of Chemical and Biomolecular Engineering, Korea Advanced Institute of Science and Technology, 291 Daehak-ro, Yuseong-gu, Daejeon 34141, Korea

(*Received 25 March 2021 • Revised 22 June 2021 • Accepted 29 June 2021*)

Abstract−We report a quick and simple method to fabricate transparent superhydrophobic polydimethylsiloxane (PDMS) using partial combustion of PDMS by thermal convection. The fabrication process only uses PDMS as an ingredient and does not require harmful, expensive materials such as organic solvent or fluoropolymer. To make PDMS superhydrophobic, combustion reaction was used to create hierarchical structures with micro- to nano-scale roughness with low surface energy required for the fabrication of superhydrophobic surface. Combustion of PDMS surface created hydrophobic silica-containing nanoparticles. These nanoparticles are deposited on the PDMS surface, creating hierarchical nano-structures required for superhydrophobic surface. To minimize the damage from excessive heat and flame, thermal convection was used to control the degree of combustion during the fabrication process. The fabricated superhydrophobic surface showed static water contact angle of 155.6°, and contact angle hysteresis of 5°. The fabricated surface also maintained light transmittance greater than 70% of the maximum transmittance of pristine PDMS in visible light region.

Keywords: Superhydrophobic Surface, PDMS, Thermal Treatment, Thermal Convection, Silica Nanoparticle

INTRODUCTION

A superhydrophobic surface, a nature-inspired surface that shows static water contact angle greater than 150°, can be found in various organisms, such as lotus leaf, rose petal, insect wings, and water strider legs [1]. Superhydrophobic surface in nature usually exhibits self-cleaning property, known as lotus effect, due to small contact angle hysteresis, often smaller than 10° [2]. Due to its unique wetting properties showing high water repellency, drag reduction and self-cleaning behavior, the superhydrophobic surface has gained wide attention from both academic and industrial fields [1].

However, the application and accessibility of superhydrophobic surface are limited due to the difficulties and costs in conventional fabrication processes. There are two requirements to make superhydrophobic surface: roughness with hierarchical micro- and nano-scale structures and low surface energy. To satisfy these requirements, conventional fabrication processes of superhydrophobic surface often use harmful and expensive chemicals such as fluoropolymers [3-5] and organic solvents [4,6-8], or involve expensive equipment such as lithography [9] and chemical vapor deposition (CVD) [10,11]. To fabricate a superhydrophobic surface quickly, easy and cost-effective methods have been introduced and widely applied [8,12,13]. One of the suggested methods involves thermal treatment of materials with low surface energy. Thermal treatment method is favored due to the simple and fast fabrication procedure and no needs for specific equipment. Using this method, a superhydrophobic surface can be fabricated easily and cost-effectively [14,15].

Thermal treatment fabrication of superhydrophobic surface involves incomplete combustion of materials with low surface energy to synthesize nanoparticles that are deposited to create hierarchical structures. One of the common ingredients of thermal treatment method is silica (SiO_2) nanoparticles from the combustion of silicone elastomers and silicone oil. Silicone elastomers and silica nanoparticles have been widely utilized in surface modification for their low surface energy and chemical, mechanical and thermal stability [16,17]. Then, previous works have suggested the possibility of using combustion of silicone product to fabricate a superhydrophobic surface, reporting that silicone combustion product, a mixture of silica and short oligomers of combusted silicone, showed superhydrophobicity [14]. Since then, various methods have been suggested to fabricate a superhydrophobic surface using combustion of silicone products. Few notable works include the fabrication of transparent superhydrophobic surface by the combustion of silicone oil on glass or wafer [18], and opaque, white-colored superhydrophobic surface by the combustion of silicone elastomers such as polydimethylsiloxane (PDMS) and 1H, 1H, 2H, 2H-perfluorooctyltrichlorosilane [19].

However, conventional combustion-based fabrication methods have a difficulty in making a transparent superhydrophobic surface. Once exposed to the heat, ingredients such as silicone and hydrocarbons lose their transparency due to formation of dark-brown and black carbon soot from incomplete combustion [14,20] and/or damage from the direct exposure to the flame such as cracks or thermal shrinkage [19]. To maintain the transparency of the substrate and prevent possible damage to the surface, it is important

†To whom correspondence should be addressed.
E-mail: DoHyun.Kim@kaist.edu

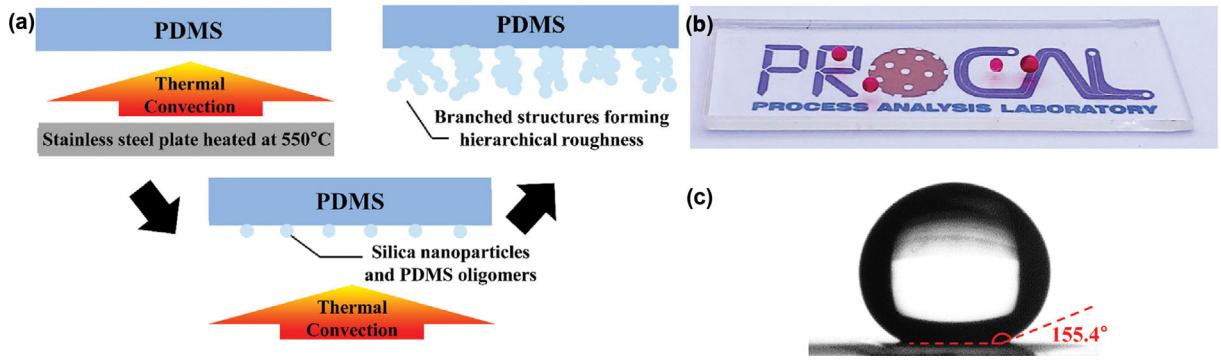

Fig. 1. (a) Schematic of the fabrication process for superhydrophobic PDMS surface. (b) The fabricated transparent superhydrophobic surface showing a logo underneath and red water drops on top of the surface. (c) Water droplet of 50 μl on the fabricated surface showing static water contact angle of 155.4°.

to control the degree of combustion during the fabrication process. To minimize the damage to the surface and control the amount of soot materials deposited on the superhydrophobic surface, we applied indirect thermal treatment using thermal convection.

To fabricate a transparent superhydrophobic surface, we used partial combustion of polydimethylsiloxane (PDMS). PDMS elastomer has been widely used in microfluidics and lithography as a flexible substrate due to its high reliability in making replicas, transparency, simple and fast processing method at relatively low temperature, thermal and chemical stability and biocompatibility [21]. PDMS is characterized by its silicon and oxygen backbone. The silicon-oxygen backbone not only increases thermal and chemical stability, but also gives affinity to other silicon based materials such as glass, silicone oil, silica, and silicon wafer [18,22]. Another powerful advantage of PDMS is its simple, easy, and fast curing process with mild reaction condition. One can easily make solid PDMS elastomer of any shape using commercial PDMS elastomer kit composed of base and curing agent. Though PDMS may not be the most cost-effective material to work with, the low difficulty in handling of the materials and curing process made PDMS one of the most widely used materials [23]. Using PDMS as a substrate for superhydrophobic surface, anyone could easily gain access to the superhydrophobic surface and its benefits.

In this work, we introduce a simple method to fabricate transparent superhydrophobic surface on PDMS using convective heat flow. The fabrication only involves PDMS, steel plate and heat source, and it only takes 1 min to finish the fabrication process. Because PDMS is not directly exposed to the flame, the degree of combustion done on the PDMS surface can be easily controlled. Using this process, transparent superhydrophobic surface could be easily realized on PDMS surface within the matter of a minute.

EXPERIMENTAL

1. Fabrication of Superhydrophobic Surface

To prepare pristine polydimethylsiloxane (PDMS), Sylgard 184 elastomer base and curing agent (Dow Corning) are used. Sylgard 184 base is mixed with curing agent in a mass ratio of 10 : 1, respectively. This PDMS mixture was set in a vacuum for 10 minutes to degas any air bubbles trapped inside. Then, the mixture was cured in the oven at 70 °C for 1 hour.

For the partial combustion of PDMS surface, indirect thermal treatment using convective heat flow was used. Stainless steel plate with thickness of 1 mm was heated to 550 °C inside a fume hood, using a gas burner (butane burner, acquired from KOVEA). Then, PDMS was placed 5 mm above the heated steel plate. The plate temperature and the distance between a heated plate and PDMS were empirically chosen and fixed to minimize the damage to the PDMS surface. After exposure to the heat for 1 min, PDMS was slowly removed from the heated plate to avoid deformation from sudden temperature change. The schematic of fabrication process is shown in Fig. 1(a).

2. Effect of Exposure Time on the PDMS Surface

To verify the effect of the exposure time on the heated plate for the combustion of PDMS surface, the fabrication process was repeated with varying exposure time on the heated plate. Additional samples were fabricated with the exposure time of 20, 30, 40, 50, 90, and 120 seconds.

3. Characterization of the Fabricated Surface

Static water contact angle and contact angle hysteresis of pristine PDMS, the fabricated superhydrophobic surface, and samples with different exposure time were measured using a contact angle analyzer (Phoenix 300, SEO). Static contact angle was measured using the sessile drop method [24]. Contact angle hysteresis was measured by subtracting advancing contact angle and receding contact angle of dynamic contact line. To compare the transparency of the fabricated surface with pristine PDMS, ultraviolet-visible (UV-vis) spectroscopy (Lambda 1050, Perkin Elmer) was used to measure the transmittance over the wavelength range from 300 nm to 800 nm. Scanning electron microscopy (SEM, Magellan 400, FEI) was used to analyze the surface morphology of the fabricated superhydrophobic surface. Change in chemical composition on the PDMS surface was analyzed using X-ray photoelectron spectroscopy (XPS, Sigma Probe, Thermo VG Scientific).

RESULTS AND DISCUSSION

1. Superhydrophobicity of the Fabricated Surface

Following the fabrication procedure, the PDMS surface successfully became superhydrophobic while maintaining its transparency.

As shown in Fig. 1(b), the surface-treated PDMS was transparent enough to transmit the image underneath the PDMS. Also, unlike previously reported work using combustion of PDMS, partially combusted PDMS surface showed no visible signs of damage or defects on the surface, maintaining the transparency and relative uniformity of the surface [19]. Fig. 1(c) shows a water droplet placed on the fabricated superhydrophobic surface. The surface-treated PDMS shows static water contact angle of 155.6±2.3°, and contact angle hysteresis of 5.2. This suggests that transparent superhydrophobic surface with Cassie-Baxter wetting state, a heterogeneous wetting state characterized by low roll-off angle and low contact angle hysteresis, was successfully fabricated on the surface of PDMS by partial combustion using thermal treatment [2,25]. Water droplets on the fabricated surface could easily slide and roll off due to low contact angle hysteresis.

2. Transparency of the Fabricated Surface

For quantitative analysis of the transparency of the surface-treated PDMS, UV-vis spectroscopy was used to measure the relative transmittance of the fabricated surface. Because transmittance of polymer film varies depending on the thickness of polymer film, intensity of transmittance was normalized for more intuitive comparison. Because PDMS is a transparent polymer, relative transmittance was normalized by setting the maximum transmittance of pristine PDMS to be 100%. UV-vis spectra in Fig. 2 show the normalized result of UV-vis spectroscopy at the wavelength from 300 nm to 800 nm. For the visible light region from the wavelength of 400 nm to 750 nm, the transmittance of surface-treated superhydrophobic surface was greater than 70% of relative transmittance, and greater than 80% of the transmittance of pristine PDMS at the given wavelength. Also, sudden decrease in the transmittance at the ultraviolet light region below the wavelength of 400 nm suggests the presence of UV light absorbing substances. This suggests that the combustion of PDMS created silica nanoparticles, as silica nanoparticles and silica containing materials also absorb UV and visible light below the wavelength of 400 nm [26].

3. Surface Morphology of the Fabricated Surface

Surface morphology is an important factor affecting the wettability of the surface. To make a material superhydrophobic, hierarchical structure in micro-and nano-scale is required to increase the roughness of surface. Using SEM, the surface morphology of the fabricated superhydrophobic PDMS surface was visualized as shown in Fig. 3. Pristine PDMS, as shown in Fig. 3(a), does not have any notable structure or roughness. However, after the thermal treatment, branched and web-like structure grew on the surface of PDMS, providing micro-scale roughness on the surface of superhydrophobic PDMS as shown in Fig. 3(b). These structures are composed of smaller nanoparticles that are interconnected with each other as shown in Fig. 3(c). These nanoparticles with diameter around 30-60 nm created nano-scale roughness.

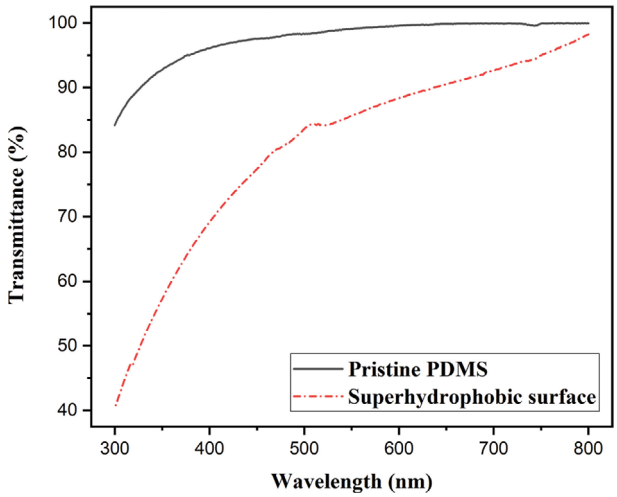

Fig. 2. UV-vis spectra of pristine PDMS and superhydrophobic PDMS. The data are normalized to set the maximum transparency of pristine PDMS to be 100%.

As described in Fig. 1(a), superhydrophobicity of the heat-treated PDMS surface was provided by the surface morphology with hierarchical structure. It has been reported that PDMS elastomers were decomposed into short PDMS oligomers and fumed silica particles as the result of combustion [14,17,18]. When exposed to oxygen, fumed silica and oxidized PDMS oligomers are combined with each other, forming silica-containing nanoparticles [17,18]. These nanoparticles are then deposited on PDMS surface, forming a branched, web-like structure as depicted in Fig. 3(b). The change in surface morphology after the thermal treatment provides a hierarchical rough structure of micro- to nano-scale, which is one of the requirements for a superhydrophobic surface.

4. Effect of Partial Combustion on the Chemical Composition of Surface

To observe any chemical change on the PDMS surface, XPS

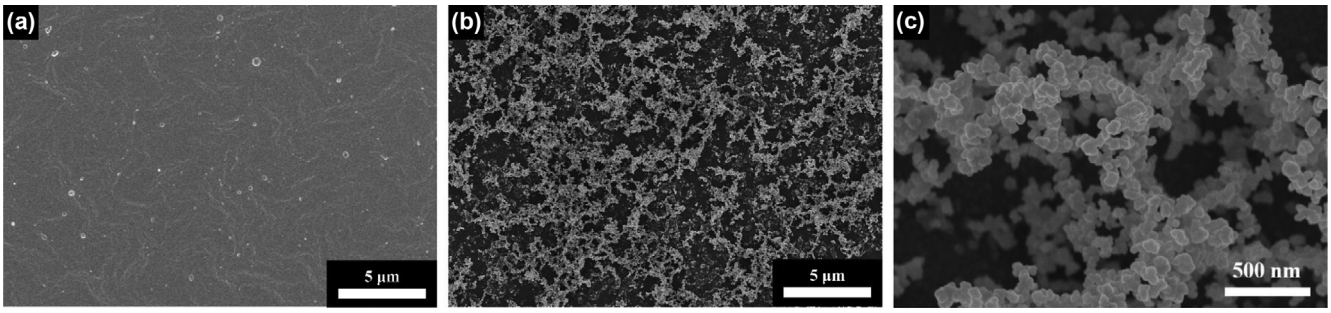

Fig. 3. SEM images of (a) pristine PDMS and (b) surface-treated transparent superhydrophobic PDMS, magnified by 5,000 times. SEM images of branched structures magnified by (c) 50,000 times.

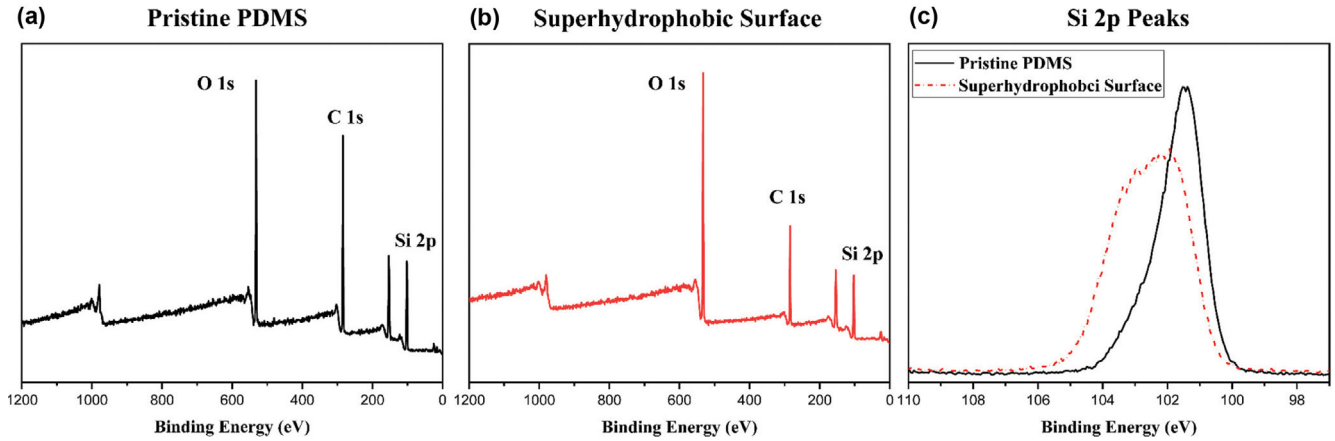

Fig. 4. XPS spectra of (a) pristine PDMS and (b) the fabricated superhydrophobic surface. (c) Si 2p peaks of both spectra are plotted together to observe the chemical change of the surface.

analysis was used to characterize the chemical composition of the branched structures. XPS surveys for pristine PDMS and superhydrophobic PDMS are shown in Fig. 4(a) and (b). Because PDMS is composed of carbon, oxygen and silicon, C 1s, O 1s, and Si 2p peaks are clearly visible on the survey. As the result of combustion reaction, the intensity of the O 1s peak increased and the intensity of the C 1s peak decreased in superhydrophobic surface compared to the pristine PDMS. This is due to the combustion reaction of PDMS, where

$$[(CH_3)_2SiO]_n+O_2\rightarrow SiO_2+CO_2+H_2O \quad (1)$$

Since carbon dioxide and water vapor are present in gaseous form at high temperature,the only product remaining on the surface is silica, and unreacted or partially reacted PDMS and PDMS oligomers. The relative increase in oxygen content and decrease in carbon content show that the combustion reaction created silica on PDMS surface.

For the detailed investigation on the chemical composition of surface structure, Si 2p peaks of pristine PDMS and surface-treated PDMS were compared with each other in Fig. 4(c). For organic silicon compound such as PDMS and other silicon carbides, Si 2p peak appears at the binding energy around 102 eV, while silica (SiO_2) shows Si 2p peak at the binding energy of 103.5 eV [27]. As shown in Fig. 4(c), pristine PDMS showed Si 2p peak near 101.6 eV, agreeing with the literature value of organic silicon peak. However, for surface-treated PDMS, Si 2p peak became broader and shifted toward the binding energy of 103.5 eV. The shift and broadening of the Si 2p peak for superhydrophobic PDMS suggests two peaks at 103.6 eV and 101.9 eV are present instantaneously. This suggests that silicon element is present in two forms: silicon oxide showing a peak at 103.6 eV, and organic silicon showing a peak at 101.9 eV, indicating that the surface structures are composed of both silica and PDMS. Although silicon dioxide is produced as the result of combustion reaction, unreacted or partially reacted hydrophobic PDMS oligomers are also present inside the nanoparticles that serve as the building blocks of surface structure. This result agrees with the results from previous works using silicone as an ingredient for superhydrophobic surface [14,18]. PDMS oligomers inside surface structures are also responsible for the hydrophobicity of the surface structure, because pure silicon dioxide is hydrophilic by itself and cannot provide the low surface energy required for the superhydrophobicity. Without PDMS oligomers present inside the surface structure, the thermally treated PDMS cannot become superhydrophobic.

5. Effect of Heat Exposure Time on the Fabricated Superhydrophobic PDMS Surface

To find the effect of the exposure time on the heated plate for the combustion of PDMS surface, the fabrication process was repeated with varying exposure time on the heated plate. The static contact angle and contact angle hysteresis of samples with different exposure time were measured and shown in Fig. 5. Contact angle of pristine PDMS was 110.2±4.5°, and contact angle hysteresis 41.5°. After being exposed to heat, the static contact angle starts to increase, while contact angle hysteresis starts to decrease. The static contact angle increased to 121.4±8.2°, 134.2±5.9° and 140.8±5.1°, while contact angle hysteresis decreased to 41.5°, 38.2° and 18.7° for 20, 30, 40 seconds after the exposure, respectively. After

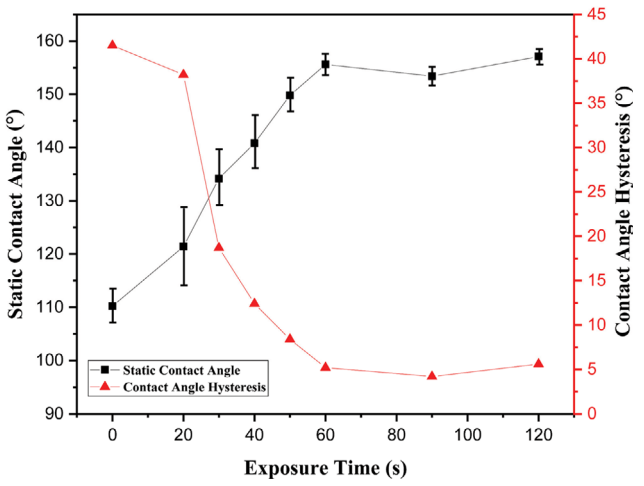

Fig. 5. Change in static contact angle and contact angle hysteresis on heat-treated PDMS surface.

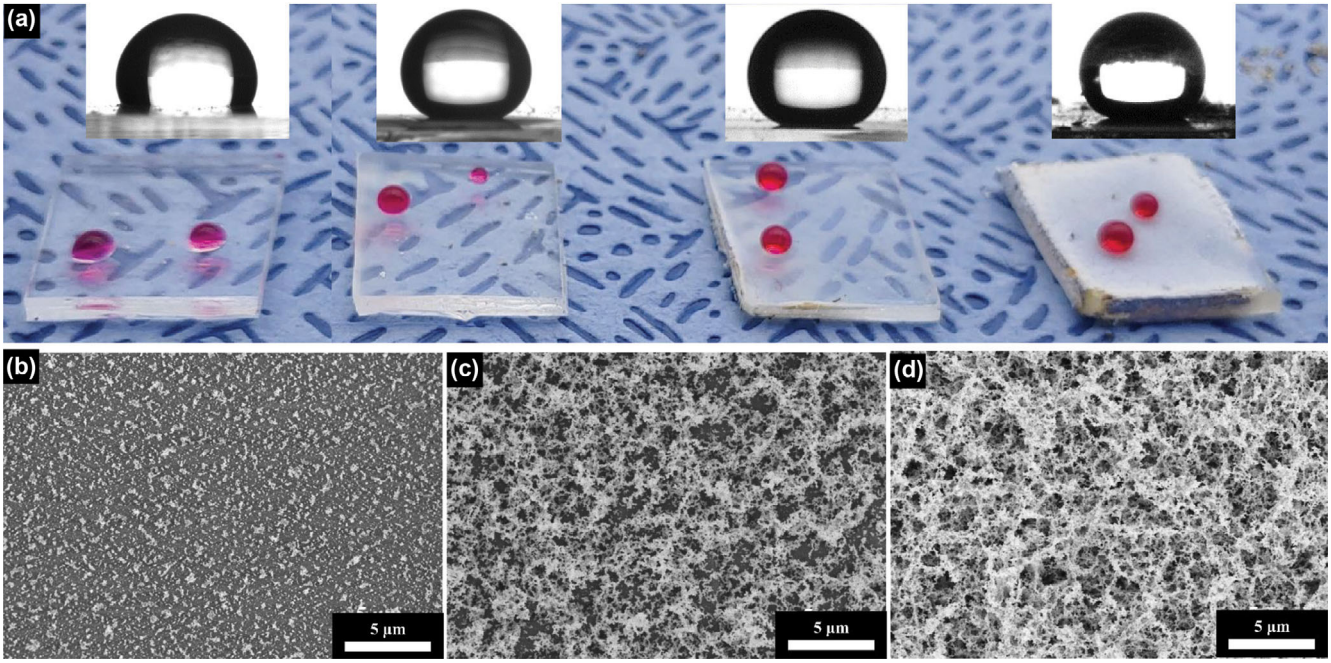

Fig. 6. (a) Photograph of samples thermally treated for 30 seconds, 60 seconds, 90 seconds, and 120 seconds from left to right, and their contact angle. SEM images of samples thermally treated for (b) 30 seconds, (c) 90 seconds, and (d) 120 seconds, magnified 5,000 times.

50 seconds of exposure, the static contact angle started to reach the superhydrophobic regime of 149.8±5.9° and contact angle hysteresis of 8.4°. Then, after 60 seconds, the static water contact angle became 155.6±2.3°, and contact angle hysteresis, 5.2° as mentioned previously. At this point, the heat-treated PDMS surface became completely superhydrophobic and additional heat treatment did not affect the contact angle much, showing static contact angle of 153.4±2.1° and 157.1±2.2°, and contact angle hysteresis of 4.2° and 5.6° for 90 and 120 seconds of exposure, respectively.

However, the transparency of the superhydrophobic PDMS was greatly affected by exposure time after 60 seconds. Fig. 6(a) is a photograph of the samples with exposure time of 30, 90, and 120 seconds. With exception of the sample with exposure time of 30 seconds, the other two samples showed superhydrophobicity as shown in Fig. 6(a). However, unlike the transparent superhydrophobic PDMS previously shown in Fig. 1(b), the superhydrophobic PDMS became more opaque and unclear. Especially for the sample with exposure time of 120 seconds, the PDMS surface turned completely white, while showing dark brown burnt edges on its sides. White color resulted from the silica containing nanoparticles, whereas dark brown coloration came from the incomplete decomposition of PDMS, leaving dark-colored hydrocarbons [14]. The combustion reaction of PDMS also decomposed and shortened the backbone of PDMS polymer chain, causing the PDMS substrate to become brittle. While the degree of combustion did not affect the superhydrophobicity of the surface after 60 seconds of thermal treatment, the combustion greatly affected the transparency of the superhydrophobic PDMS. Therefore, exposure time around 60 seconds is favored; otherwise, the superhydrophobic PDMS becomes too opaque and loses its transparency.

SEM images of these samples explain why too much combustion caused the superhydrophobic PDMS to lose its transparency. As previously shown in Fig. 3(a), pristine PDMS showed no major roughness on the surface. However, partial combustion of PDMS surface caused silica nanoparticles and PDMS oligomers to be deposited on the surface of heat-treated PDMS. SEM image of surface with 30 seconds of heat treatment in Fig. 6(b) shows the growth of micro-structures on PDMS surface. The bare PDMS surface is represented as darker color, while silica contacting branched structures are represented with white and brighter color. As the combustion reaction continued, branched structures started to cover more portion of the PDMS surface as shown in Fig. 3(b) and Fig. 6(c). After 120 seconds, the branched structures completely covered the PDMS surface, showing no dark gray color of bare PDMS surface on Fig. 6(d) and causing the surface to become opaque and white as shown in Fig. 6(a).

CONCLUSION

Using thermal convection, the degree of combustion of PDMS elastomer could be easily controlled, and transparent superhydrophobic surface was successfully fabricated with relatively simple and fast fabrication procedures. Partial combustion reaction changed the surface morphology by producing silica-containing nanoparticles and depositing them on the surface to make web-like branched structures. These branched structures made of hydrophobic nanoparticles provided hierarchical roughness from micro- to nanoscale, rendering the surface superhydrophobic. The fabricated surface exhibited superhydrophobicity with Cassie-Baxter wetting state, showing static water contact angle around 155.6° and contact angle hysteresis around 5.2°, while maintaining its transparency. The relative transmittance of superhydrophobic PDMS was greater than

70% in visible light regime. Using this fabrication method, we expect the application of transparent superhydrophobic PDMS elastomers in various engineering fields.

ACKNOWLEDGEMENT

This work was supported by the National Research Foundation of Korea (NRF) through Basic Science Research Program funded by the Ministry of Science and ICT (No. 2018R1A2A3075668).

SUPPORTING INFORMATION

Additional information as noted in the text. This information is available via the Internet at http://www.springer.com/chemistry/journal/11814.

REFERENCES

1. Y. Zhang, H. Xia, E. Kim and H. Sun, *Soft Matter*, **8**, 11217 (2012).
2. W. Barthlott and C. Neinhius, *Planta*, **202**, 1 (1997).
3. M. Yang, W. Liu, C. Jiang, S. He, Y. Xie and Z. Wang, *Carbohydr. Polym.*, **197**, 75 (2018).
4. I. A. Larmour, S. E. J. Bell and G. C. Saunders, *Angew. Chem., Int. Ed.*, **46**, 1710 (2017).
5. K. Ravi, W. L. Sulen, C. Bernard, Y. Ichikawa and K. Ogawa, *Surf. Coat. Technol.*, **373**, 17 (2019).
6. Y. Ma, X. Cao, X. Feng, Y. Ma and H. Zou, *Polymer*, **48**, 7455 (2007).
7. X. Xu, Z. Zhang and W. Liu, *Colloids Surf., A*, **341**, 21 (2009).
8. C. H. Xue, S. T. Jia, J. Zhang and J. Z. Ma, *Sci. Technol. Adv. Mater.*, **11**, 1 (2010).
9. Y. H. Sung, Y. D. Kim, H. Choi, R. Shin, S. Kang and H. Lee, *Appl. Surf. Sci.*, **349**, 169 (2015).
10. S. Rezaei, I. Manoucheri, R. Moradian and B. Pourabbas, *Chem. Eng. J.*, **252**, 11 (2014).
11. L. Xu, J. Deng, Y. Guo, W. Wang, R. Zhang and J. Yu, *Text. Res. J.*, **89**, 1853 (2019).
12. J. Li, X. Liu, Y. Ye, H. Zhou and J. Chen, *Appl. Surf. Sci.*, **258**, 1772 (2011).
13. J. Zhu, H. Wan and X. Hu, *Prog. Org. Coat.*, **100**, 56 (2016).
14. L. Shen, W. Qiu, B. Liu and Q. Guo, *RSC Adv.*, **4**, 56259 (2014).
15. X. Deng, L. Mammen, H. J. Butt and D. Vollmer, *Science*, **335**, 67 (2012).
16. A. Eifert, D. Paulssen, S. N. Varankkottu, T. Baier and S. Hardt, *Adv. Mater. Interfaces*, **1**, 1300138 (2014).
17. R. G. Karunakaran, C. H. Lu, Z. Zhang and S. Yang, *Langmuir*, **27**, 4594 (2011).
18. K. Seo, M. Kim, S. Seok and D. H. Kim, *Colloids Surf., A*, **492**, 110 (2016).
19. X. Tian, S. Shaw, K. R. Lind and L. Cademartiri, *Adv. Mater.*, **28**, 3677 (2016).
20. R. Iqbal, B. Majhy and A. K. Sen, *ACS Appl. Mater. Interfaces*, **9**, 31170 (2017).
21. J. C. MacDonald, D. C. Duffy, J. R. Anderson, D. T. Chiu, H. Wu, O. J. A. Schueller and G. M. Whitesides, *Electrophoresis*, **21**, 27 (2000).
22. G. Graffius, F. Bernardoni and A. Y. Fadeev, *Langmuir*, **30**, 14797 (2014).
23. R. Mukhopadhyay, *Anal. Chem.*, **79**, 3248 (2007).
24. K. Seo, M. Kim, J. K. Ahn and D. H. Kim, *Korean J. Chem. Eng.*, **32**, 2394 (2015).
25. A. B. D. Cassie and S. Baxter, *Trans. Faraday Soc.*, **40**, 546 (1944).
26. C. D. Marshall, J. A. Speth and S. A. Payne, *J. Non-Cryst. Solids*, **212**, 59 (1997).
27. T. N. Taylor, *J. Mater. Res.*, **4**, 189 (1989).